

Adiabatic and nonadiabatic spin-transfer torques in the current-driven magnetic domain wall motion

Jun-ichiro Kishine

Department of Basic Sciences, Kyushu Institute of Technology, Kitakyushu 804-8550, Japan

A. S. Ovchinnikov

Department of Physics, Ural State University, Ekaterinburg 620083, Russia

(Received 4 February 2010; published 6 April 2010)

A consistent theory to describe the correlated dynamics of quantum-mechanical itinerant spins and semiclassical local magnetization is given. We consider the itinerant spins as quantum-mechanical operators, whereas local moments are considered within classical Lagrangian formalism. By appropriately treating fluctuation space spanned by basis functions, including a zero-mode wave function, we construct coupled equations of motion for the collective coordinate of the center-of-mass motion and the localized zero-mode coordinate perpendicular to the domain wall plane. By solving them, we demonstrate that the correlated dynamics is understood through a hierarchy of two time scales: Boltzmann relaxation time τ_{el} , when a nonadiabatic part of the spin-transfer torque appears, and Gilbert damping time τ_{DW} , when adiabatic part comes up.

DOI: 10.1103/PhysRevB.81.134405

PACS number(s): 75.60.-d, 72.25.Pn, 72.15.Gd

I. INTRODUCTION

Spin torque transfer (STT) process is expected to revolutionize the performance of memory device due to nonvolatility and low-power consumption. To promote this technology, it is essential to make clear the nature of the current-driven domain wall (DW) motion.^{1,2} Recent theoretical³⁻¹⁰ and experimental^{11,12} studies have disclosed that the STT consists of two vectors perpendicular to the local magnetization $\mathbf{m}(x)$ and can be written in general as $\mathbf{N} = c_1 \partial_x \mathbf{m} + c_2 \mathbf{m} \times \partial_x \mathbf{m}$.³ The c_1 and c_2 terms, respectively, come from adiabatic^{1,4} and nonadiabatic⁵ processes between conduction electrons and local magnetization, and the terminal velocity of a DW is controlled by not c_1 but small c_2 term. The origin of the c_2 term is ascribed to the spatial mistracking of spins between conduction electrons and local magnetization.⁵ Behind appearance of the c_2 term is the so-called transverse spin accumulation (TSA) of itinerant electrons generated by the electric current.^{6,7} Now, any consistent theory should explain how the adiabatic and nonadiabatic STT come up starting with microscopic model. In particular, it should be made clear how the TSA caused by the nonadiabatic STT eventually leads to translational motion of the whole DW.

In this paper, we arrange existing physical ideas in a rigorous mathematical frame and give a closed formula to compute the domain wall velocity as a function of injected current density [Eqs. (23) and (24)]. In Sec. II, we present a model. In Sec. III, we derive coupled equations of motion for the collective coordinate of the center-of-mass motion and the localized zero-mode coordinate perpendicular to the domain wall plane. Then, we solve them to demonstrate that the correlated dynamics is understood through a hierarchy of Boltzmann relaxation time τ_{el} and Gilbert damping time τ_{DW} . We conclude our results in Sec. IV. Some technical details are left to appendices.

II. MODEL

We consider a single head-to-head Néel DW through a magnetic nanowire with an easy x axis and a hard z axis.

Free electrons travel along the DW axis (x axis). We describe a local spin by a semiclassical vector $\mathbf{S} = S\mathbf{n} = S(\sin \theta \cos \varphi, \sin \theta \sin \varphi, \cos \theta)$ where $S = |\mathbf{S}|$ and the polar coordinates θ and φ are assumed to be slowly varying functions of one-dimensional coordinate x [Fig. 1(a)]. The DW formation is described by the Hamiltonian (energy per unit area) in the continuum limit

$$\mathcal{H}_{DW} = \frac{JS^2}{2a} \int_{-\infty}^{\infty} dx [(\partial_x \mathbf{n})^2 - \lambda^{-2} \hat{n}_x^2 + \kappa^{-2} \hat{n}_z^2], \quad (1)$$

where a is the cubic lattice constant, J is the ferromagnetic exchange strength, $\lambda = \sqrt{J/2K}$ and $\kappa = \sqrt{J/2K_{\perp}}$, respectively, represent the single-ion easy and hard axis anisotropies measured in the length dimension. The stationary Néel wall ($\theta_0 = \pi/2$) is described by $\mathbf{n}_0 = (\cos \varphi_0, \sin \varphi_0, 0)$ with

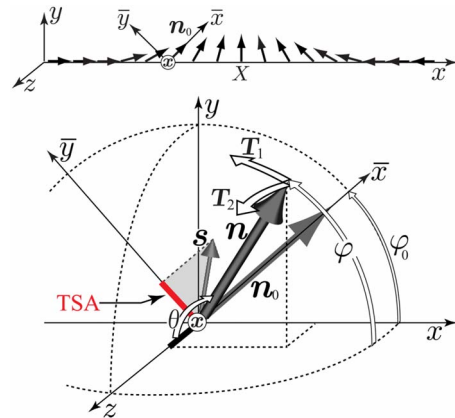


FIG. 1. (Color online) (a) Stationary configuration of local spins (\mathbf{n}_0) associated with a single Néel wall. Laboratory frames x , y , and z and local frames \bar{x} , \bar{y} , and \bar{z} are indicated. (b) Schematic view of the TSA of itinerant spin \mathbf{s} and the OPZA of local spin \mathbf{n} . These magnetic accumulations, respectively, cause the nonadiabatic torque \mathbf{T}_2 and adiabatic torque \mathbf{T}_1 .

$\varphi_0(x) = 2 \arctan(e^{x/\lambda})$. In the infinite continuum system, the DW configuration has continuous degeneracy labeled by the center of mass position, X , of the DW. This degeneracy apparently leads to *rigid* translation of the DW, i.e., $\mathbf{n}_0(x) \rightarrow \mathbf{n}_0(x-X)$.¹³ As explicitly shown below, however, the translation in off-equilibrium accompanies *internal deformation* of the DW.

The creation operator of a conduction electron is written in a spinor form as $c^\dagger(x) = [c^\dagger_\uparrow(x), c^\dagger_\downarrow(x)]$. By performing the local gauge transformation $c(x) = \hat{U}(x)\bar{c}(x)$ with the unitary operator $\hat{U}(x) = e^{i\hat{\sigma}_z\varphi_0(x)/2}$ ($\hat{\sigma}_z$ is a Pauli matrix) the quantization axis becomes parallel to the local spin located at x . Assuming $|a\partial_x\varphi_0(x)| \approx a/\lambda \ll 1$, i.e., wall thickness is much larger than atomic lattice constant, this procedure leads to the single-particle Hamiltonian

$$\mathcal{H}_{el} = \frac{\hbar^2}{2m^*a} \int_{-\infty}^{\infty} dx \left[\frac{1}{2} |\partial_x \bar{c}|^2 + i(\partial_x \bar{c}^\dagger) \hat{A}_z \bar{c} \right] + \text{c.c.}, \quad (2)$$

where the effective mass of the conduction electron is m^* . The SU(2) gauge field^{8,14} is introduced as $\hat{A}_z \equiv i^{-1} \hat{U}^{-1} \partial_x \hat{U} = -(\partial_x \varphi_0) \hat{\sigma}_z / 2$. The conduction electrons are assumed to interact with the local spins by an s - d coupling represented in the form

$$\mathcal{H}_{sd} = -\frac{J_{sd}}{a^3} \int_{-\infty}^{\infty} dx \hat{s}(x) \cdot \mathbf{S}(x-X), \quad (3)$$

where \hat{s} and $\mathbf{S} = S\mathbf{n}$ are, respectively, the spins of itinerant and localized electrons. We treat $\hat{s}(x) = \frac{1}{2} c^\dagger \hat{\boldsymbol{\sigma}} c$ as fully quantum-mechanical operator while \mathbf{n} is a semiclassical vector.

III. DYNAMICS

A. Boltzmann relaxation

Let switch on the electric field E at $t=0$. We introduce the Boltzmann relaxation time τ_{el} and the number density of the conduction electrons $f_{k\sigma}$ in the state k, σ . We assume that the deviation from equilibrium Fermi-Dirac distribution $f_0(\varepsilon_{k\sigma}) = \{\exp[(\varepsilon_{k\sigma} - \mu)/k_B T] + 1\}^{-1}$ is small, where $\varepsilon_{k\sigma}$ ($\sigma = \uparrow, \downarrow$) is the single-particle energy and μ is the chemical potential. Using standard Boltzmann kinetic equation with relaxation-time approximation,⁶ the distribution function is written as

$$f_{k\sigma} \approx f_0(\varepsilon_{k\sigma}) + eE\tau_{el} v_{k\sigma} \frac{\partial f_0(\varepsilon_{k\sigma})}{\partial \varepsilon_{k\sigma}}, \quad (4)$$

where the electron charge is $-e$ and the spin-dependent velocity is $v_{k\sigma} \equiv \hbar^{-1} \partial \varepsilon_{k\sigma} / \partial k$. The spin dependence of $\varepsilon_{k\sigma}$ originates from the SU(2) gauge fields $(\hat{A}_z)_{\uparrow\uparrow}$ and $(\hat{A}_z)_{\downarrow\downarrow}$. In the process of approaching to stationary current flowing state around the time $t \sim \tau_{el}$, as we will show explicitly, the statistical average of the conduction electron's spin component perpendicular to the local quantization axis \bar{x} accumulates and acquires finite value. As schematically depicted in Fig. 1(b), this process is exactly the TSA. The TSA causes an additional magnetic field acting on the local spins and exert the nonadiabatic torque on the local spins.

B. Local spin dynamics

Next we formulate dynamics of the local spins coupled with the conduction electrons. We introduce the $\delta\theta(x, t)$ (out-of-plane) and $\delta\varphi(x, t)$ (in-plane) fluctuations of the local spins around the stationary DW configuration $\mathbf{n}_0(x)$, i.e., $\varphi(x) = \varphi_0(x-X) + \delta\varphi(x-X)$ and $\theta(x) = \pi/2 + \delta\theta(x-X)$. The terms ‘‘out-of-plane’’ and ‘‘in-plane’’ are determined with respect to the DW plane. In addition, we emphasize that X is not at the stage a dynamical variable but just a parameter.

By expanding \mathcal{H}_{DW} up to the second order with respect to the $\delta\theta$ and $\delta\varphi$, $\mathcal{H}_{DW}[\theta, \varphi] = \mathcal{H}_{DW}[\theta_0, \varphi_0] + \delta\mathcal{H}_\theta + \delta\mathcal{H}_\varphi$, one find that the Hilbert space of the fluctuations is spanned by the orthogonal basis functions v_q and u_q

$$\delta\varphi(x) = \int_{-\infty}^{\infty} dq \eta_q(t) v_q(x), \quad \delta\theta(x) = \int_{-\infty}^{\infty} dq \xi_q(t) u_q(x), \quad (5)$$

where η_q and ξ_q are the time-dependent eigenmode coordinates.¹⁵

These eigenfunctions are determined from the Schrödinger-type equations with the Pöschl-Teller potential¹⁶

$$\frac{JS^2}{2} \left[-\partial_x^2 - \frac{2}{\lambda^2} \frac{1}{\cosh^2(x/\lambda)} + \frac{1}{\lambda^2} \right] v_q(x) = \varepsilon_q^\varphi v_q(x), \quad (6a)$$

$$\frac{JS^2}{2} \left[-\partial_x^2 - \frac{2}{\lambda^2} \frac{1}{\cosh^2(x/\lambda)} + \frac{1}{\lambda^2} + \frac{1}{\kappa^2} \right] u_q(x) = \varepsilon_q^\theta u_q(x) \quad (6b)$$

and diagonalize the fluctuation parts $\delta\mathcal{H}_\theta$ and $\delta\mathcal{H}_\varphi$. We note that the fluctuations become rotationally invariant when the hard axis anisotropy $K_\perp = 0$.

Both θ and φ modes consist of a single bound state (*zero mode*) and continuum states (*spin-wave modes*). The dimensionless zero-mode wave functions are given by $u_0(x) = v_0(x) = \Phi_0(x)$, where

$$\Phi_0(x) \equiv \sqrt{\frac{a\lambda}{2}} \partial_x \varphi_0(x) = \sqrt{\frac{a}{2\lambda}} \frac{1}{\cosh(x/\lambda)} \quad (7)$$

with the corresponding energies $\varepsilon_0^\theta = JS^2/(2\kappa^2)$ and $\varepsilon_0^\varphi = 0$, respectively. The normalization is determined through $a^{-1} \int_{-\infty}^{\infty} dx |\Phi_0(x)|^2 = 1$. Since to excite the out-of-plane (θ) zero mode costs finite energy gap ε_0^θ coming from the hard-axis anisotropy, we call it ‘‘quasizero mode.’’

The spin-wave states

$$v_q(x) = u_q(x) = \sqrt{\frac{a}{2\pi}} \frac{e^{iqx}}{\sqrt{(1+\lambda^2q^2)}} \left[-iq\lambda + \tanh\left(\frac{x}{\lambda}\right) \right] \quad (8)$$

are normalized by $a^{-1} \int_{-\infty}^{\infty} dx v_q^*(x) v_{q'}(x) = \delta(q-q')$ and with the same condition for $u_q(x)$.¹⁷ These states have energy dispersions $\varepsilon_q^\varphi = \frac{1}{2} JS^2 (q^2 + \lambda^{-2})$ and $\varepsilon_q^\theta = \frac{1}{2} JS^2 (q^2 + \lambda^{-2} + \kappa^{-2})$. Because the zero (quasizero) mode and the spin-wave states are orthogonal to each other and separated by the anisotropy gaps, the spin-wave modes are totally irrelevant for a low-

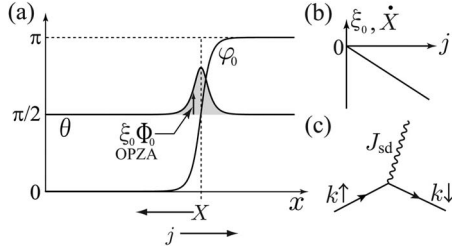


FIG. 2. (a) Spatial profile of the polar angles $\varphi(x,t) = \varphi_0[x-X(t)]$ and $\theta(x,t) = \pi/2 + \xi_0(t)\Phi_0[x-X(t)]$ in the flowing current state. (b) Linear dependence of ξ_0 and $\dot{X}(t)$ on the current density j . (c) Single-particle propagation (represented by solid line) with spin flip process by the s - d interaction (represented by wavy line) which leads to the STT.

energy effective theory. Therefore, we ignore their contribution from now on.

In order to obtain a correct local spin dynamics, one has to regard the parameter X as a dynamical variable $X(t)$ and replace the zero mode (Goldstone) coordinate η_0 with $X(t)$.¹⁸ Following this idea, the zero/quasizero mode fluctuations should be presented as

$$\varphi(x,t) = \varphi_0[x-X(t)], \quad (9)$$

$$\theta(x,t) = \pi/2 + \xi_0(t)\Phi_0[x-X(t)]. \quad (10)$$

Equation (10) is a key ingredient of the paper (see discussion in Appendix A), which has been early suggested by us in the studies of a chiral helimagnet.¹⁹ That is to say, we naturally include the out-of-plane quasizero (OPZ) mode, in addition to the in-plane (φ) zero mode replaced by $X(t)$. The zero-mode wave function $\Phi_0[x-X(t)]$ serves as the basis function of the θ fluctuations localized around the center of the DW and $\xi_0(t)$ is the OPZ *coordinate* (for detail discussion, see Sec. IV). Now, our effective theory is fully described by two dynamical variables $X(t)$ and $\xi_0(t)$ which play a role of physical coordinates along the Hilbert space of the orthogonal θ and φ fluctuations. Below, we prove that $\xi_0(t) \neq 0$ only for nonequilibrium flowing current state arising at $E \neq 0$ [Fig. 2(a)].

C. Equations of motion of the DW

Now, we construct an effective Lagrangian $\mathcal{L} = \mathcal{L}_{\text{DW}} + \mathcal{L}_{sd}$ to describe the DW motion and resultant equations of motion (EOM). Using Eqs. (9) and (10), the local spin counterpart is given by $\mathcal{L}_{\text{DW}} = \frac{\hbar S}{a^3} \int_{-\infty}^{\infty} dx (\cos \theta - 1) \dot{\varphi} - \mathcal{H}_{\text{DW}}$ explicitly written as

$$\mathcal{L}_{\text{DW}} = \frac{\hbar S}{a^3} \left(\sqrt{\frac{2a}{\lambda}} \xi_0 + \pi \right) \dot{X} - \frac{JS^2}{2\kappa^2} \xi_0^2. \quad (11)$$

To understand the effect of the s - d coupling, it is useful to note $\mathbf{n}[\theta_0 + \delta\theta, \varphi_0 + \delta\varphi] = \mathbf{n}_0 - e_z \delta\theta - \mathbf{n}_0 \delta\theta^2/2$, where we dropped $\delta\varphi$ because this degree of freedom is eliminated by the global gauge fixing. We have thus s - d Lagrangian

$$\mathcal{L}_{sd} = a^{-3} J_{sd} S (\mathcal{F}_0 - S_{\parallel} \xi_0^2/2), \quad (12)$$

where

$$\mathcal{F}_0[X(t)] \equiv \int_{-\infty}^{\infty} dx \hat{\mathbf{n}}_0[x-X(t)] \cdot \langle \mathbf{s}(x,t) \rangle$$

and

$$S_{\parallel}[X(t)] \equiv \int_{-\infty}^{\infty} dx \{ \Phi_0[x-X(t)] \}^2 \mathbf{n}_0[x-X(t)] \cdot \langle \mathbf{s}(x,t) \rangle.$$

Finally, to take account of dissipative dynamics, we use the Rayleigh dissipation function $\mathcal{W}_{\text{Rayleigh}} = \frac{\alpha \hbar S}{2 a^3} \int_{-\infty}^{\infty} dx \dot{\mathbf{n}}^2$ explicitly written as

$$\mathcal{W}_{\text{Rayleigh}} = \frac{\alpha \hbar S}{2 a^3} \left(a \dot{\xi}_0^2 + \frac{2}{\lambda} \dot{X}^2 \right), \quad (13)$$

where α is the Gilbert damping parameter. It is simple to write down the Euler-Lagrange-Rayleigh equations, $d(\partial L / \partial \dot{q}_i) / dt - \partial L / \partial q_i = -\partial W / \partial \dot{q}_i$, for two dynamical variables $q_1 = X$ and $q_2 = \xi_0$. In linear order the EOM have the form

$$\hbar \sqrt{\frac{2a}{\lambda}} \dot{\xi}_0 + J_{sd} \mathcal{T}_{\perp} = -2\alpha \frac{\hbar}{\lambda} \dot{X}, \quad (14a)$$

$$-\hbar \sqrt{\frac{2a}{\lambda}} \dot{X} + \left(\frac{a^3 JS}{\kappa^2} + J_{sd} S_{\parallel} \right) \xi_0 = -\alpha \hbar a \dot{\xi}_0, \quad (14b)$$

where the quantities

$$\mathcal{T}_{\perp} \equiv -\frac{\partial \mathcal{F}_0}{\partial X} = \int_{-\infty}^{\infty} dx \partial_x \varphi_0[x-X(t)] \langle \bar{s}_y(x) \rangle, \quad (15a)$$

$$S_{\parallel} \equiv \int_{-\infty}^{\infty} dx \Phi_0^2[x-X(t)] \langle \bar{s}_x(x) \rangle, \quad (15b)$$

respectively give the nonadiabatic STT and longitudinal spin accumulation.⁷ The statistical average of the conduction electron's spin component is denoted by $\langle \dots \rangle$. The gauge-transformed spin variables are introduced by $\bar{s}(x) = \hat{U}^{-1}[x-X(t)] \hat{s}(x) \hat{U}[x-X(t)]$ which has local quantization axis tied to the local spin at the position of $x-X(t)$.

To obtain Eq. (15a), we use the relations

$$\partial_x \mathbf{n}_0[x-X(t)] = -\partial_x \varphi_0(x) \mathbf{e}_z \times \mathbf{n}_0[x-X(t)]$$

and

$$\langle \bar{s}_y \rangle = -\langle \hat{s}_x \rangle \sin \varphi_0 + \langle \hat{s}_y \rangle \cos \varphi_0.$$

It is also to be noted that we ignored the term $\partial S_{\parallel} / \partial X$. This simplification is legitimate for the case of small s - d coupling.

The relation (15a) implies that upon a switching of an external electric field the TSA, $\langle \bar{s}_y \rangle$, along the local \bar{y} axis appears and creates a spin torque, which causes a precession of the local magnetic moment around the \bar{y} axis and consequently produces a finite deviation of the polar angle $\delta\theta = \theta - \theta_0$. We call this process out-of-plane quasizero-mode accumulation (OPZA) schematically depicted in Fig. 1(b). This effect is physically similar to an emergence of a demagnetization field phenomenologically introduced by Döring, Kittel, and Becker,²⁰ and Slonczewski.¹

Formally, it means that a nonzero coordinate $\xi_0(t)$ arises and reaches a finite terminal value ξ_0^* . Indeed, the coupled equations of motion in Eqs. (14a) and (14b) are readily solved to give the relaxational behavior

$$\xi_0 = \xi_0^*(1 - e^{-t/\tau_{\text{DW}}}), \quad (16)$$

$$V \equiv \dot{X} = V^*(1 - e^{-t/\tau_{\text{DW}}}), \quad (17)$$

where

$$\xi_0^* = -\frac{1}{\alpha} \frac{\sqrt{a\lambda/2} J_{sd} \mathcal{T}_\perp}{\alpha(a^3 J_s \kappa^{-2} + J_{sd} \mathcal{S}_\parallel)} \approx -\alpha^{-1} \sqrt{\frac{\lambda}{2a}} \left(\frac{\kappa}{a}\right)^2 \frac{J_{sd} \mathcal{T}_\perp}{J_s} \quad (18)$$

and the terminal velocity of the DW is

$$V^* = -\frac{\lambda}{2\alpha\hbar} J_{sd} \mathcal{T}_\perp. \quad (19)$$

The relaxation time of the DW magnetization, τ_{DW} , is given by

$$\tau_{\text{DW}} = \hbar a \frac{\alpha^{-1} + \alpha}{\kappa^{-2} a^3 J_s + J_{sd} \mathcal{S}_\parallel} \approx \alpha^{-1} \left(\frac{\kappa}{a}\right)^2 \frac{\hbar}{J_s}. \quad (20)$$

These results clearly show that the DW magnetization try to relax through the Gilbert damping toward the direction of the newly established precession axis. We stress that without the OPZ coordinate ξ_0 in Eqs. (14a) and (14b), only the terminal velocity is available and the transient relaxational dynamics is totally lost.

It should be noted that when K_\perp is zero ($\kappa \rightarrow \infty$), the quazero mode coordinate ξ_0 diverges [see Eq. (18)] that results in an infinite inertial mass of the DW. To grapple with a physical meaning of this result, we stress that the rotational symmetry around the DW axis is recovered at $K_\perp = 0$, and fluctuations associated with this rotation diverges. That is to say, the zero K_\perp causes continuous degeneracy and the system possesses gauge degrees of freedom concerning how to choose the origin θ_0 of the θ angle. The θ_0 fixing corresponds to spontaneously broken symmetry. On the other hand, a finite K_\perp (our case) causes an energy gap and the gauge symmetry is broken from the beginning, therefore to make an infinitesimal rotation of the DW around an axis costs a finite energy. Due to this mechanism, the θ fluctuations, or ξ_0 , do not diverge and a finite mass of the DW appears. In this sense, the energy gap ε_0^θ of the quazero mode caused by K_\perp plays a role of ‘‘protector’’ of the inertial DW motion.

D. Hierarchy in the relaxational processes

The important consequence of the OPZA [Eq. (18)] is an emergence of the finite out-of-plane (z) component of the local spin

$$n_z(x, t) = \cos \theta \approx \frac{1}{2\alpha} \left(\frac{\kappa}{a}\right)^2 \frac{J_{sd}}{J_s} \frac{1}{\cosh\{[x - X(t)]/\lambda\}} \mathcal{T}_\perp. \quad (21)$$

The resultant constituent $\mathcal{S}_\perp = S e_z n_z(x, t)$ provides the Slonczewsky-type demagnetization field and contributes

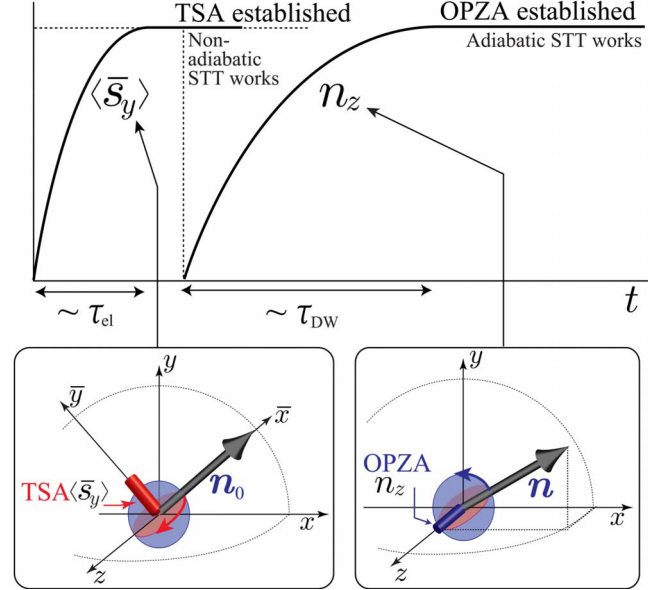


FIG. 3. (Color online) The whole processes of establishing the nonadiabatic and adiabatic STTs. After switching on the electric field at $t=0$, the inequilibrium process toward the stationary flowing current state with time scale $t \approx \tau_{\text{el}}$ (Boltzmann relaxation) causes the finite TSA $\langle \bar{s}_y \rangle$ and resultant nonadiabatic torque, \mathcal{T}_\perp . Then, around the time scale of $t \approx \tau_{\text{el}} + \tau_{\text{DW}}$ (Gilbert relaxation), the whole system reaches *nonequilibrium but stationary* state with the OPZA (n_z) being established and macroscopic rotation of the DW spins being realized.

to the adiabatic torque $\mathbf{T}_1 = c_1 \partial_x \mathbf{n}(x) = c_1 (\partial_x \varphi_0) (-\sin \varphi_0, \cos \varphi_0, 0)$. At the head-to-head interface of the DW boundary, $\varphi_0 = \pi/2$ and $\mathbf{T}_1 = c_1 (\partial_x \varphi_0) (-1, 0, 0)$, i.e., the adiabatic torque rotates the local spin to counterclockwise direction when the electric current flows in the opposite (1,0,0) direction. As it is clear from the above discussion, this adiabatic torque is established *after* the stationary flowing current [$\mathbf{j} = (ne^2 \tau_{\text{el}} / m^*) \mathbf{E}$] state establishes the nonadiabatic torque, \mathcal{T}_\perp . Within the time scale of order $t \approx \tau_{\text{el}} + \tau_{\text{DW}}$, the whole system (including conduction electrons and DW) reaches a *nonequilibrium but stationary* state. In this state, the DW magnetizations continuously feel the OPZA with n_z being given by Eq. (21) and macroscopically rotate around it. This process exactly corresponds to stationary translation of the DW. The mechanism is schematically shown in Fig. 3.

E. Master formula for the DW velocity under the electric current

In the following, we compute the explicit form of \mathcal{T}_\perp and \mathcal{S}_\parallel . The details of the calculations are relegated to Appendix B. The derivation leads to

$$\mathcal{T}_\perp = \frac{1}{2} \int_{-\pi/a}^{\pi/a} dk \operatorname{Re} G_{k_\uparrow, k_\downarrow}^<(t, t), \quad (22a)$$

$$\mathcal{S}_\parallel = \frac{a}{2\pi} \int_{-\pi/a}^{\pi/a} dk \operatorname{Im} G_{k_\uparrow, k_\downarrow}^<(t, t). \quad (22b)$$

These quantities are computed by using the lesser component of the path-oriented Green’s function

$G_{k\sigma,k'\sigma'}^<(t,t')=i\langle\bar{c}_{k'\sigma'}^\dagger(t')\bar{c}_{k\sigma}(t)\rangle$, where t (t') is defined on the upper (lower) branch of the Keldysh contour.²¹

Since \mathcal{S}_\parallel does not play an essential role, we pay attention to the more important quantity \mathcal{T}_\perp . To find the lesser Green's function in Eq. (22a) we use the technique based on EOM for nonequilibrium (Keldysh) Green's functions.²² An advantage of the straightforward method is an absence of a graphical analysis, which depends on a specific form of a Hamiltonian. Within the approach the s - d coupling is perturbatively treated and the Dyson equation is written down (see Appendix C). Then, we truncate the Dyson equation in the framework of the Born approximation that results in

$$G_{k\uparrow,k\downarrow}^<(t,t)=-i\frac{J_{sd}}{2}\frac{f_{k\uparrow}-f_{k\downarrow}}{\varepsilon_{k\uparrow}-\varepsilon_{k\downarrow}-i0}. \quad (22c)$$

In the linear order, the s - d coupling causes a single spin flip process [Fig. 2(c)] and contributes to off-diagonal electron spin component.

To obtain the explicit form of $\varepsilon_{k\sigma}$, we write the single-particle Hamiltonian (2) in Fourier space and obtain $\mathcal{H}_{el}=\mathcal{H}_0+\mathcal{H}_{\text{gauge}}$, where \mathcal{H}_0 represents free conduction and $\mathcal{H}_{\text{gauge}}$ comes from the second term in Eq. (2). By retaining only momentum-conserving process, we have $\mathcal{H}_{el}=\sum_{k,\sigma}\varepsilon_{k\sigma}\bar{c}_{k\sigma}^\dagger\bar{c}_{k\sigma}$, where $\varepsilon_{k\uparrow,\downarrow}=\hbar^2(k\mp\delta k)^2/2m^*$, and the shift of the Fermi wave numbers due to the background DW is given by $\delta k=\pi/(2a)$.

Combining together Eqs. (19) and (22a) we obtain the master formula for the DW velocity. First, using Eqs. (4), (22c), and (22a), we obtain the explicit form of the STT which points in the z direction, $\mathbf{T}_2=\mathcal{T}_\perp e_z$

$$\mathcal{T}_\perp=\frac{1}{4}\frac{J_{sd}}{k_B T}\frac{1}{\cosh^2[(\varepsilon_0-\mu)/2k_B T]}\frac{j}{j_0}. \quad (23)$$

Here, $j_0=4ne\hbar/(\pi am^*)$ and $\varepsilon_0=\hbar^2\pi^2/(8m^*a^2)$ corresponds to the chemical potential at half-filling. Then, we reach from Eq. (19) the master formula which establishes a relation between the current density and the DW terminal velocity

$$V^*=-\frac{1}{8\alpha}\frac{\lambda J_{sd} J_{sd}}{\hbar k_B T}\frac{1}{\cosh^2[(\varepsilon_0-\mu)/2k_B T]}\frac{j}{j_0}. \quad (24)$$

As shown in Fig. 2(b), there is no threshold for the velocity that is consistent with the result obtained by Thiaville *et al.*¹⁰ A standard choice of the parameters, $j_0\approx 10^{16}$ [A m⁻²], $\lambda=10^{-8}$ [m], $\alpha=10^{-2}$, and $j\approx 10^{11}$ [A m⁻²] gives the rough estimate $V^*\approx -100(J_{sd}/k_B T)^2$ [m/s]. Of course, to pursuit a more quantitative result one needs a numerical estimation of \mathcal{T}_\perp based on a real band structure.

IV. CONCLUSIONS

In this paper, we present a consistent theory to describe a correlated dynamics of quantum-mechanical itinerant spins and semiclassical local magnetization when an electric current flows through a magnetic nanowire with a single head-to-head Néel domain wall inside. The most essential point made clear is the relaxation process of the DW dynamics governed by the Boltzmann relaxation followed by the Gil-

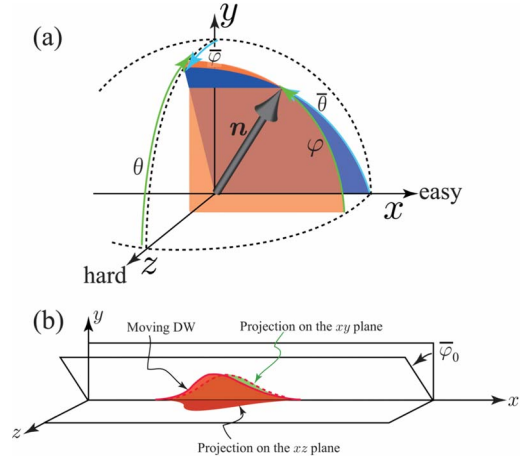


FIG. 4. (Color online) (a) Walker's choice of polar coordinates. (b) Profile of a moving domain wall and its projections onto the xy plane (in-plane) and xz plane (out-of-plane). When $\bar{\varphi}=\bar{\varphi}_0$ =small constant, the profile on the xz plane coincides with our quasizero-mode wave function.

bert damping in hierarchical manner (Fig. 3). As summarized in Figs. 2(a) and 2(b), it is crucial to recognize that the OPZ coordinate ξ_0 acquires a finite value (accumulation) only for a current flowing state which is nonequilibrium but stationary. This is the case when a dynamical relaxation leads to finite accumulation of physical quantities. Although an essential role of the sliding mode to describe a localized spin dynamics has been pointed out before^{8,13} as well as an importance of out-of-plane canting of the local spins,^{1,8} the OPZA presented in the study has not been discussed before. For example, the sliding motion in Ref. 13 does not contain internal deformation of the DW. An appearance of the OPZA in the current-flowing nonequilibrium state is an outcome of a time-reversal symmetry breaking by the electric field.

ACKNOWLEDGMENTS

J.K. acknowledges Grant-in-Aid for Scientific Research (C) (Grant No. 19540371) from the Ministry of Education, Culture, Sports, Science and Technology, Japan.

APPENDIX A: QUASIZERO-MODE COORDINATE ξ_0 AS A DYNAMICAL ORDER PARAMETER

In this section, we comment a physical meaning of the expansion given by Eqs. (10), which constitutes one of the essential points of the paper. In particular, we focus on new moments of the treatment in comparison with that of originally suggested by Walker^{23,24} and utilized by many authors.^{8,25}

An apparent discrepancy emerges due to different parametrization through the polar coordinates. Walker *et al.* used the choice^{23,24} $n_x=\cos\bar{\theta}$, $n_y=\sin\bar{\theta}\cos\bar{\varphi}$, and $n_z=\sin\bar{\theta}\sin\bar{\varphi}$ via the angles shown in Fig. 4(a). The stationary wall solution is given by $\bar{\varphi}=0$, $\bar{\theta}=\bar{\theta}_0(x)=2\arctan(e^{x/\lambda})$ that results in $n_{0x}=-\tanh(x/\lambda)$, $n_{0y}=\cosh^{-1}(x/\lambda)=\lambda\partial_x\bar{\theta}_0(x)$, and $n_{0z}=0$. Then, a local spin dynamics is described by the

Lagrangian density $\mathcal{L} = \hbar S \bar{\varphi}_t \cos \bar{\theta} - \frac{S^2}{2} [J(\bar{\theta}_x^2 + \sin^2 \bar{\theta} \bar{\varphi}_x^2) + K_\perp \sin^2 \bar{\theta} \sin^2 \bar{\varphi} - K \cos^2 \bar{\theta}]$ together with the Rayleigh dissipation function. To solve the Euler-Lagrange-Rayleigh equation of motion derived from this Lagrangian, Walker assumes a rigid translation of the domain wall²⁴

$$\bar{\varphi} = \bar{\varphi}_0 (\text{small const}), \quad \bar{\theta} = \bar{\theta}_0 [x - X(t)]. \quad (\text{A1})$$

At the moment, we note that a dynamics of $\bar{\varphi}$ angle is totally neglected. However, in a presence of the Gilbert damping, it is impossible to retain the finite $\bar{\varphi}$. Instead, it is natural to expect that $\bar{\varphi}$ relaxes eventually to zero. An adoption of Walker's assumption $\bar{\varphi}_t = 0$ results in

$$\bar{\theta}_{0t} = \frac{K_\perp S}{2\hbar} \sin \bar{\theta}_0 \sin 2\bar{\varphi}_0, \quad (\text{A2})$$

which plays a crucial role in Walker's theory because there is no chance to relate $\bar{\varphi}_0$ with the wall velocity \dot{X} without this equation.

By using Eq. (A1) we obtain for small $\bar{\varphi}_0$

$$n_x = \cos \bar{\theta}_0 [x - X(t)], \quad (\text{A3a})$$

$$n_y \simeq \sin \bar{\theta}_0 [x - X(t)] = \lambda \partial_x \bar{\theta}_0 [x - X(t)], \quad (\text{A3b})$$

$$n_z \simeq \bar{\varphi}_0 \sin \bar{\theta}_0 [x - X(t)] = \lambda \bar{\varphi}_0 \partial_x \bar{\theta}_0 [x - X(t)]. \quad (\text{A3c})$$

From Eq. (A3c) it is clearly seen that the in-plane ($\bar{\theta}$) and out-of-plane ($\bar{\varphi}$) modes are inevitably *coupled* with each other even at the Gaussian level.

On the other hand, in *our* choice of polar coordinates (see Fig. 1), the Gaussian fluctuations described by Eqs. (9) and (10) lead to

$$n_x \simeq \cos \varphi_0 [x - X(t)], \quad (\text{A4a})$$

$$n_y \simeq \sin \varphi_0 [x - X(t)], \quad (\text{A4b})$$

$$n_z \simeq -\sqrt{a\lambda/2} \xi_0(t) \partial_x \varphi_0 [x - X(t)], \quad (\text{A4c})$$

Again, we stress that $\xi_0(t)$ is not a basis function but just a dynamical variable. Thus, the parametrization makes the in-plane and out-of-plane modes *independent*. Formally, Eqs. (A3c) and (A4c) have the same form as far as $\bar{\varphi}_0$ is being constant in time. Hence, our ξ_0 apparently plays the same role as $\bar{\varphi}_0$ [see Fig. 4(b)]. However, the out-of-plane and in-plane fluctuations in our treatment should be orthogonal regarding a spanning of Hilbert space, whereas Walker's choice corresponds to a "curvilinear" coordinate frame (coupled fluctuations).

A clear discrepancy is revealed in a relaxational dynamics. Without an external electric field, Eqs. (14a) and (14b) yield the relaxational dynamics $\dot{X}(t) = V_0 e^{-t/\tau}$ and $\xi_0(t) = \xi_0^* e^{-t/\tau}$ if to take \mathcal{T}_\perp and \mathcal{S}_\parallel to be zero. This result is never reached if to assume Eq. (A1).

As a conclusion, ξ_0 describes an amplitude of the OPZA and plays a role of "dynamical order parameter" which manifests itself as an appearance of physical quantities which are zero in equilibrium.²⁶

APPENDIX B: CALCULATION OF \mathcal{T}_\perp AND \mathcal{S}_\parallel

Our goal is to obtain the expressions given by Eqs. (22a) and (22b). By definition, the nonadiabatic STT is

$$\mathcal{T}_\perp = \int_{-\infty}^{\infty} dx \partial_x \varphi_0 [x - X(t)] \langle \bar{s}_y(x) \rangle.$$

Taking the Fourier transform $\bar{c}_{k\sigma}(t) = \frac{1}{\sqrt{L}} \sum_k e^{ikx} \bar{c}_\sigma(x, t)$ with L being the whole length of the magnetic wire, we obtain

$$\mathcal{T}_\perp = \frac{1}{2L} \sum_{k, k'} \int_{-\infty}^{\infty} dx \partial_x \varphi_0 [x - X(t)] \langle \bar{c}_k^\dagger \sigma^y \bar{c}_{k'} \rangle e^{-i(k-k')x}. \quad (\text{B1})$$

Retaining only the momentum conserving processes, $k = k'$

$$\begin{aligned} \mathcal{T}_\perp &\approx \frac{1}{2L} \sum_k \int_{-\infty}^{\infty} dx \partial_x \varphi_0 [x - X(t)] \langle \bar{c}_k^\dagger \sigma^y \bar{c}_k \rangle \\ &= \frac{\pi}{2L} \sum_k \langle \bar{c}_k^\dagger \sigma^y \bar{c}_k \rangle = \frac{1}{4} \int_{-\pi/a}^{\pi/a} dk \langle \bar{c}_k^\dagger \sigma^y \bar{c}_k \rangle. \end{aligned} \quad (\text{B2})$$

The longitudinal spin accumulation transforms in a similar way

$$\begin{aligned} \mathcal{S}_\parallel &= \int_{-\infty}^{\infty} dx \Phi_0^2 [x - X(t)] \langle \bar{s}_x(x) \rangle \\ &= \frac{1}{2L} \sum_{k, k'} \int_{-\infty}^{\infty} dx \Phi_0^2 [x - X(t)] \langle \bar{c}_k^\dagger \sigma^x \bar{c}_{k'} \rangle e^{-i(k-k')x}. \end{aligned} \quad (\text{B3})$$

Picking up the terms with $k = k'$ we get

$$\begin{aligned} \mathcal{S}_\parallel &\approx \frac{1}{2L} \sum_k \int_{-\infty}^{\infty} dx \Phi_0^2 [x - X(t)] \langle \bar{c}_k^\dagger \sigma^x \bar{c}_k \rangle \\ &= \frac{a}{2L} \sum_k \langle \bar{c}_k^\dagger \sigma^x \bar{c}_k \rangle = \frac{a}{4\pi} \int_{-\pi/a}^{\pi/a} dk \langle \bar{c}_k^\dagger \sigma^x \bar{c}_k \rangle. \end{aligned} \quad (\text{B4})$$

Plugging the relationship $\langle \bar{c}_k^\dagger \sigma^\alpha \bar{c}_k \rangle = -i \text{Tr}[\hat{G}_{k,k}^<(t, t) \sigma^\alpha]$ in Eqs. (B2) and (B4) and using the properties of the lesser Green's function $\text{Re} \hat{G}_{k\uparrow, k\downarrow}^<(t, t) = -\text{Re} \hat{G}_{k\downarrow, k\uparrow}^<(t, t)$ and $\text{Im} \hat{G}_{k\uparrow, k\downarrow}^<(t, t) = \text{Im} \hat{G}_{k\downarrow, k\uparrow}^<(t, t)$ [see Eq. (C13)] we reproduce eventually the results of Eqs. (22a) and (22b).

APPENDIX C: KELDYSH GREEN'S FUNCTION

In the EOM approach the Hamiltonian of the system is splitted into two parts $H = H_0 + H_1$, where $H_0 = H_{\text{kin}}$ describes noninteracting electrons, and the perturbation $H_1 = H_{sd}$ represents interaction of the electrons with the local moments. It is initially supposed that $H_1 = 0$ at $t = -\infty$. When H_1 is switched on adiabatically, the s - d interaction starts to affect an electron transport.

The nonequilibrium Green's function is defined by

$$i \langle \langle A(t_a) B(t_b) \rangle \rangle = \text{Tr} \{ \rho_0 T [A(t_a) B(t_b) S_C] \}, \quad (\text{C1})$$

where ρ_0 stands for the density matrix of the initially noninteracting system and T denotes the time-ordering operator.

The subscript C indicates the time loop (Keldysh contour) and the time-loop S matrix is given by

$$S_C = T_c \left\{ \exp \left[-i \int_C H_1(t) dt \right] \right\}.$$

This Green's function contains information on retarded, advanced, and lesser Green's functions.

The EOM for the nonequilibrium Green's functions in Eq. (C1) has the form

$$\begin{aligned} \langle\langle A(t_a)B(t_b) \rangle\rangle &= g_a(t_a - t_b) \langle\langle D(t_b) \rangle\rangle \\ &+ \int_C dt g_a(t_a - t) \langle\langle C(t)B(t_b) \rangle\rangle. \end{aligned} \quad (C2)$$

The definition includes the anticommutator $D(t) = [A(t), B(t)]_+$ and the commutator $C(t) = [A(t), H_1(t)]$. The single-particle time-loop Green's function g_a is defined for different relative orders of t_1 and t_2 on the Keldysh contour

$$ig_a(t_2 - t_1) = \begin{cases} \frac{f_a(t_2 - t_1)}{1 + F_a} & t_2 > c t_1 \\ -\frac{F_a f_a(t_2 - t_1)}{1 + F_a} & t_2 < c t_1. \end{cases} \quad (C3)$$

The coefficients F_a and f_a are obtained from the relationships $A(t_a)\rho_0 = F_a\rho_0 A(t_a)$, and $A(t_a) = \alpha_1, \dots, \alpha_n f_a(t_a)$, where α represent either creation or annihilation operators.

To estimate the electron spin components in nonequilibrium state we need the contour-ordered Green's function

$$G_{k\sigma; k'\sigma'}(t_a, t_b) = \langle\langle a_{k\sigma}(t_a) a_{k'\sigma'}^\dagger(t_b) \rangle\rangle \quad (C4)$$

with the EOM

$$\begin{aligned} \langle\langle a_{k\sigma}(t_a) a_{k'\sigma'}^\dagger(t_b) \rangle\rangle &= g_{k\sigma}(t_a - t_b) \delta_{kk'} \delta_{\sigma\sigma'} - \frac{J_{sd}S}{2} \\ &\times \sum_{\sigma_1} \sigma_{\sigma\sigma_1}^x \int_C dt g_{k\sigma}(t_a - t) \langle\langle a_{k\sigma_1}(t) a_{k'\sigma'}^\dagger(t_b) \rangle\rangle. \end{aligned} \quad (C5)$$

Using the equilibrium density matrix $\rho_0 = \exp(-\beta \sum_{k\sigma} \epsilon_{k\sigma} a_{k\sigma}^\dagger a_{k\sigma}) / \text{Tr}\{\exp(-\beta \sum_{k\sigma} \epsilon_{k\sigma} a_{k\sigma}^\dagger a_{k\sigma})\}$ we obtain the coefficient

$$F_{k\sigma} = e^{-\beta \epsilon_{k\sigma}} \quad (C6)$$

and the form for the single-particle time-loop Green's function

$$ig_{k\sigma}(t_2 - t_1) = \begin{cases} (1 - f_{k\sigma}) e^{-i\epsilon_{k\sigma}(t_2 - t_1)} & t_2 > c t_1 \\ -f_{k\sigma} e^{-i\epsilon_{k\sigma}(t_2 - t_1)} & t_2 < c t_1, \end{cases} \quad (C7)$$

where $f_{k\sigma} = (e^{\beta \epsilon_{k\sigma}} + 1)^{-1}$ is the Fermi-distribution function.

Since, there is four different combinations for the times t_2 and t_1 located on either of two branches C_+ (the upper) and C_- (the lower) of the Keldysh contour, the contour-ordered Green's function in Eq. (C7) contains four different functions. The greater ($t_2 > c t_1$) and the lesser ($t_2 < c t_1$) Green's functions are, respectively,

$$ig_{k\sigma}^>(t_2 - t_1) = (1 - f_{k\sigma}) e^{-i\epsilon_{k\sigma}(t_2 - t_1)}, \quad (C8)$$

$$ig_{k\sigma}^<(t_2 - t_1) = -f_{k\sigma} e^{-i\epsilon_{k\sigma}(t_2 - t_1)}, \quad (C9)$$

whereas the retarded (advanced) Green's functions are given by

$$\begin{aligned} g_{k\sigma}^R(t_2 - t_1) &= \theta(t_2 - t_1) [g_{k\sigma}^>(t_2 - t_1) - g_{k\sigma}^<(t_2 - t_1)] \\ &= -i\theta(t_2 - t_1) e^{-i\epsilon_{k\sigma}(t_2 - t_1)}, \end{aligned} \quad (C10)$$

$$\begin{aligned} g_{k\sigma}^A(t_2 - t_1) &= \theta(t_1 - t_2) [g_{k\sigma}^<(t_2 - t_1) - g_{k\sigma}^>(t_2 - t_1)] \\ &= i\theta(t_1 - t_2) e^{-i\epsilon_{k\sigma}(t_2 - t_1)}. \end{aligned} \quad (C11)$$

Following the Langreth theorem, the integration over the loop in Eq. (C5) can be changed to integration along the real-time axis.²⁷ To evaluate the electron spin density, we need to take the lesser component of the contour-ordered Green's functions

$$\begin{aligned} G_{k\sigma; k'\sigma'}^<(t_a, t_b) &= g_{k\sigma}^<(t_a - t_b) \delta_{kk'} \delta_{\sigma\sigma'} - \frac{J_{sd}S}{2} \sum_{\sigma_1} \sigma_{\sigma\sigma_1}^x \int_{-\infty}^{+\infty} dt g_{k\sigma}^R(t_a - t) G_{k\sigma_1; k'\sigma'}^<(t - t_b) \\ &- \frac{J_{sd}S}{2} \sum_{\sigma_1} \sigma_{\sigma\sigma_1}^x \int_{-\infty}^{+\infty} dt g_{k\sigma}^<(t_a - t) G_{k\sigma_1; k'\sigma'}^A(t - t_b). \end{aligned} \quad (C12)$$

In the first order Born approximation this gives

$$G_{k\sigma; k'\sigma'}^<(t_a, t_b) \approx if_{k\sigma} e^{-i\epsilon_{k\sigma}(t_a - t_b)} \delta_{kk'} \delta_{\sigma\sigma'} - i \frac{J_{sd}S}{2} \frac{f_{k\sigma} e^{-i\epsilon_{k\sigma}(t_a - t_b)} - f_{k\sigma'} e^{-i\epsilon_{k\sigma'}(t_a - t_b)}}{\epsilon_{k\sigma} - \epsilon_{k\sigma'} - i\delta} \delta_{kk'} \sigma_{\sigma\sigma'}^x \quad (C13)$$

that provides the result in Eq. (22c).

- ¹J. C. Slonczewski, *J. Magn. Magn. Mater.* **159**, L1 (1996).
- ²L. Berger, *Phys. Rev. B* **54**, 9353 (1996).
- ³M. D. Stiles and A. Zangwill, *Phys. Rev. B* **66**, 014407 (2002).
- ⁴Ya. B. Bazaliy, B. A. Jones, and S.-C. Zhang, *Phys. Rev. B* **57**, R3213 (1998).
- ⁵S. Zhang and Z. Li, *Phys. Rev. Lett.* **93**, 127204 (2004).
- ⁶J. Xiao, A. Zangwill, and M. D. Stiles, *Phys. Rev. B* **73**, 054428 (2006).
- ⁷S. Zhang, P. M. Levy, and A. Fert, *Phys. Rev. Lett.* **88**, 236601 (2002).
- ⁸G. Tatara and H. Kohno, *Phys. Rev. Lett.* **92**, 086601 (2004).
- ⁹G. Tatara, H. Kohno, and J. Shibata, *Phys. Rep.* **468**, 213 (2008).
- ¹⁰A. Thiaville, Y. Nakatani, J. Miltat, and Y. Suzuki, *Europhys. Lett.* **69**, 990 (2005).
- ¹¹S. Petit, C. Baraduc, C. Thirion, U. Ebels, Y. Liu, M. Li, P. Wang, and B. Dieny, *Phys. Rev. Lett.* **98**, 077203 (2007).
- ¹²Z. Li, S. Zhang, Z. Diao, Y. Ding, X. Tang, D. M. Apalkov, Z. Yang, K. Kawabata, and Y. Huai, *Phys. Rev. Lett.* **100**, 246602 (2008).
- ¹³S. E. Barnes and S. Maekawa, *Phys. Rev. Lett.* **95**, 107204 (2005).
- ¹⁴G. E. Volovik, *J. Phys. C* **20**, L83 (1987).
- ¹⁵Y. Le Maho, J.-V. Kim, and G. Tatara, *Phys. Rev. B* **79**, 174404 (2009).
- ¹⁶S. Flügge, *Practical Quantum Mechanics* (Springer-Verlag, Berlin, 1971).
- ¹⁷J. M. Winter, *Phys. Rev.* **124**, 452 (1961).
- ¹⁸R. Rajaraman, *Solitons and Instantons* (North-Holland, Amsterdam, 1982).
- ¹⁹The out-of-plane quasizero mode was discussed in the context of chiral helimagnet by the present authors: I. G. Bostrem, J. Kishine, and A. S. Ovchinnikov, *Phys. Rev. B* **77**, 132405 (2008); **78**, 064425 (2008); I. G. Bostrem, J. Kishine, R. V. Lavrov, and A. S. Ovchinnikov, *Phys. Lett. A* **373**, 558 (2009).
- ²⁰W. Döring, *Z. Naturforsch. B* **3a**, 374 (1948); R. Becker, Proceedings of the Grenoble Conference, July, 1950 (unpublished); C. Kittel, *Phys. Rev.* **80**, 918 (1950).
- ²¹L. P. Keldysh, *Zh. Eksp. Teor. Fiz.* **47**, 1515 (1964) [*Sov. Phys. JETP* **20**, 1018 (1965)].
- ²²C. Niu, D. L. Lin, and T.-H. Lin, *J. Phys.: Condens. Matter* **11**, 1511 (1999).
- ²³L. R. Walker (unpublished),; quoted in J. F. Dillon in *A Treatise on Magnetism*, edited by G. T. Rado and H. Suhl (Academic, New York, 1963), Vol. III.
- ²⁴N. L. Schryer and L. R. Walker, *J. Appl. Phys.* **45**, 5406 (1974).
- ²⁵H. Braun, J. Kyriakidis, and D. Loss, *Phys. Rev. B* **56**, 8129 (1997).
- ²⁶We remark that in the conventional Landau theory of the second-order phase transition, it is essential to distinguish the basis function and the order parameter.
- ²⁷H. Haug and A. P. Jauho, *Quantum Kinetics in Transport and Optics of Semi-conductors* (Springer-Verlag, Berlin, 1998).